Solution structure of a DNA hairpin and its disulfide cross-linked analog

Robert J. Cain[1], Erik R. P. Zuiderweg[2] and Gary D. Glick[1,2,*]

[1]Department of Chemistry and [2]Biophysics Research Division and Department of Biological Chemistry, University of Michigan, Ann Arbor, MI 48109-1055, USA

ABSTRACT

The solution structures of a 21 base long DNA hairpin derived from the ColE1 cruciform, and an analog possessing a disulfide cross-link bridging the terminal bases, have been determined by NMR spectroscopy. The 8 bp long stem of these sequences adopts a B-form helix whereas the five base long single-stranded loop appears to be flexible and cannot be represented by a unique static conformation. NOESY cross-peak volumes, proton and phosphorus chemical shifts, and both homo- and heteronuclear coupling constants for the cross-linked hairpin are virtually identical to those measured for the unmodified sequence, even for the residues that are proximal to the cross-link. These results indicate that both hairpins are structurally isomorphous. Because this cross-link can be incorporated site specifically in a sequence independent manner, and does not appear to alter native conformation, it should prove broadly applicable in studies of DNA structure and function.

INTRODUCTION

A range of chemical and enzymatic methods have been developed to introduce covalent interstrand cross-links into nucleic acids (1–14). Such cross-linked constructs have a variety of applications ranging from biophysical characterization of nucleic acid structures that are otherwise difficult to examine, to protein/drug–DNA binding studies (4,7,15). Cross-linked nucleic acids are often prepared by reaction of alkylating agents or mutagens with nucleophilic sites on the bases. However, these molecules generally display poor site-specificity and usually afford a complex mixture of cross-linked adducts (2,5,8,14). Other compounds like cisplatin (6,16), mitomycin C (17–19) and psoralen (1,4) can form lesions at unique sites, but their sequence-dependent reactivity limits their utility for engineering a broad range of site-specific cross-links.

We and others have described synthetic protocols for site-specifically modifying both DNA and RNA with disulfide cross-links (20–27). In our method, incorporation of N^3-thioethylthymidine (or N^3-thioethyluridine for RNA) at both the 3'- and 5'-ends of oligonucleotide duplexes by solid-phase synthesis, affords disulfide cross-links following mild air oxidation. Using this simple technique we have prepared cross-linked hairpins (21,22,26),

duplexes (22) and triplexes (27), and have stabilized a non-ground-state DNA conformation (22). The cross-link does not inhibit the action of modifying or restriction enzymes, and the analytical techniques that are routinely used to characterize DNA and RNA, like sequencing and footprinting, can be applied to our disulfide-modified oligonucleotides without problems (28–30).

Continued use of disulfide cross-linked nucleic acids, however, requires an understanding of the structural consequences of incorporating such modifications. The importance of determining the structure of cross-linked nucleic acids is underscored in recent studies by Wemmer which showed that a DNA–psoralen adduct possesses an altered DNA geometry (31). Here we present NMR data and the structures of two 21 base long DNA hairpins: an unmodified sequence (1) which terminates with an A and T, and a disulfide cross-linked analog (2) where the terminal bases are replaced with N^3-thioethylthymidine (Fig. 1). We selected this sequence initially because it is a high affinity target for lupus anti-DNA autoantibodies (30) and it forms an especially stable hairpin (28). As described below, NMR data clearly indicate that the cross-link in 2 does not alter the structure of this hairpin relative to 1.

MATERIALS AND METHODS

Sample preparation

Hairpins 1 and 2 were synthesized as previously described by Glick (21). For spectra measured in D_2O, the DNA was lyophilized from D_2O to remove residual traces of H_2O and was then dissolved in buffer (50 mM NaCl, 10 mM NaD_2PO_4, pH 7) to a final concentration of 1.5 mM. The spectra measured in H_2O also included 10% D_2O.

NMR spectroscopy

All NMR Spectra were measured on a Bruker AMX 500 spectrometer and were processed on a Silicon Graphics 4D/35 workstation using the FELIX software package (Biosym Technologies). Each experiment described below was performed for both 1 and 2 at 10°C. Presaturation was used to suppress the residual HOD signal for spectra measured in D_2O except for the NOESY mixing time series for which water suppression was not employed. All spectra were measured in the phase sensitive mode with TPPI phase cycling (32), except for the heteronuclear ^{31}P–^1H experiments where States phase cycling (33) was employed. Homonuclear

---

*To whom correspondence should be addressed at: Department of Chemistry, University of Michigan, 930 North University Avenue, Ann Arbor, MI 48109-1055, USA
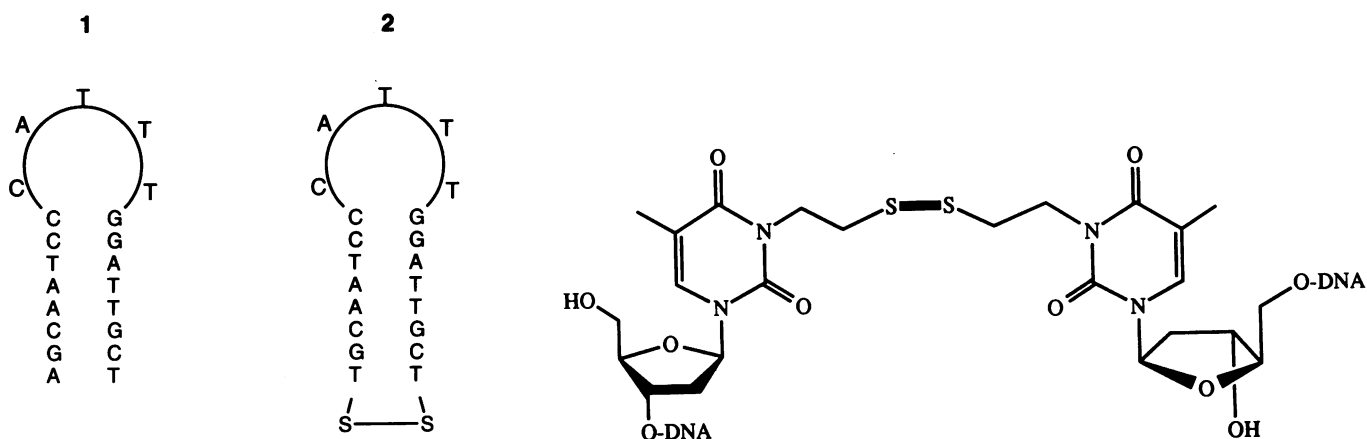
Figure 1. Sequences of 1 and 2, and the chemical structure of the disulfide cross-link.

spectra were typically measured with spectral widths of 5000 Hz in both dimensions and ~700 t1 increments of 2000 complex points. All FIDs were subjected to a time domain convolution (34) with a sinebell window to suppress the solvent signal and then apodized using shifted sine bell functions. Zero filling to at least twice the original data size was performed in both dimensions.

To assign the nonlabile protons, NOESY (τ_m = 200 ms; 35), DQF-COSY (36) and Z-filtered clean TOCSY (37,38) spectra were measured in D_2O. For the TOCSY experiment, an MLEV16 (39) isotropic mixing sequence was used with suitable delays inserted to cancel ROESY effects (40). To assign the ^{31}P resonances, a non-selective proton detected heteronuclear correlation experiment (41) was performed with a spectral width of 393 Hz in the indirect dimension and 100 t1 increments. The labile protons were assigned from NOESY spectra (τ_m = 200 ms) measured in 90% H_2O/10% D_2O. A 1-1 read pulse (42) was used to suppress the H_2O signal.

To obtain ^1H-^1H coupling constants, double and triple quantum filtered COSY spectra were measured as 700 t1 increments of 2048 complex points with 24 and 48 scans per increment, respectively. Analysis of the COSY multiplets was carried out on spectral expansions that were constructed using zero filling of at least eight times the original data size. Complementary E. COSY spectra were obtained by adding and subtracting the double and triple quantum filtered COSY spectra (43). To obtain $^3J^{31}P_{-H3'}$ values, a selective ^1H-^{31}P correlation experiment (44) was performed using an IBURP (45) shaped pulse with a spectral width of 196 Hz in the indirect dimension and 100 t1 increments. Some of the $^3J_{H3'-H4'}$ coupling constants were obtained using the convolution procedure of Titman and Keeler (46). Briefly, a COSY cross section through the H3'-H4' multiplet was convoluted with an in-phase stick doublet of trial separation (J_{trial}) and the corresponding NOESY cross section was convoluted with an anti-phase stick doublet of the same separation. The J_{trial} and the relative amplitudes of the stick doublets were then varied in a grid search procedure to find the best fit as judged by RMS difference between the convoluted multiplets.

To obtain distance constraints for the structure calculations, a series of NOESY spectra were measured in D_2O (τ_m = 15, 30, 50, 80, 125 and 200 ms) over a continuous 12 day period without solvent suppression. To reduce zero-quantum artifacts, the 15 and 30 ms mixing times were randomly varied by ± 2.5 and 3.0 ms, respectively, while the other mixing times were varied by ± 5 ms. The mixing times were varied such that each random mixing time was used for one complete phase cycle before switching to the next

value. A 2 s recycle delay was used for the above experiments and an additional 200 ms spectrum was measured under identical conditions with a 9 s recycle delay.

Data analysis

To eliminate the effect of the short recycle delay on the NOESY cross-peak volumes, the ratio of all the corresponding resolved strong peaks in the 200 ms spectra that employed both the long and short recycle delays were collected. These ratios were tabulated according to the ω-1 proton assigned to the cross-peak. The weighted average of these ratios for each ω-1 proton was then applied as a correction factor for all the NOESY cross-peaks at each mixing time. In cases where no strong cross-peak was available, an approximate correction factor was assigned based on the type of proton (i.e. aromatic or sugar).

Clearly resolved cross-peaks were integrated using the 'box method' in the FELIX software package. For cases of two overlapped cross-peaks, the volumes of the component cross-peaks were obtained using a simulation method similar to that of Prestegard (47–48). In our variation a volume normalized experimental matrix composed of two overlapped peaks is fitted to two normalized synthetic matrices containing peaks that possess the shapes and coordinates of the individual peaks which are overlapped. This fitting procedure determined the fraction of the experimental peak volume attributable to each component peak and therefore allowed the component peak volumes to be calculated. To create the synthetic peak for each component peak, ω-1 and ω-2 profile vectors were obtained from other resolved peaks. The ω-2 profile vector was taken from a row vector through a clearly resolved peak sharing the same ω-2 resonance and the ω-1 profile was taken from a column vector of a clearly resolved peak sharing the same ω-1 resonance. After the parts of the vectors away from the peak of interest were set to zero, these vectors were multiplied as matrices to produce a two dimensional matrix containing the synthetic peak.

For each assigned cross-peak, the NOE intensity was fit to equation 1:

$$V(\tau_m) = A_0 * \tau_m + A_1 * \tau^2_m + A_2 * \tau^3_m \tag{1}$$

where V is the NOESY peak volume and τ_m is the NOESY mixing time. The initial slopes of the fitting, A_0, were then assumed to be
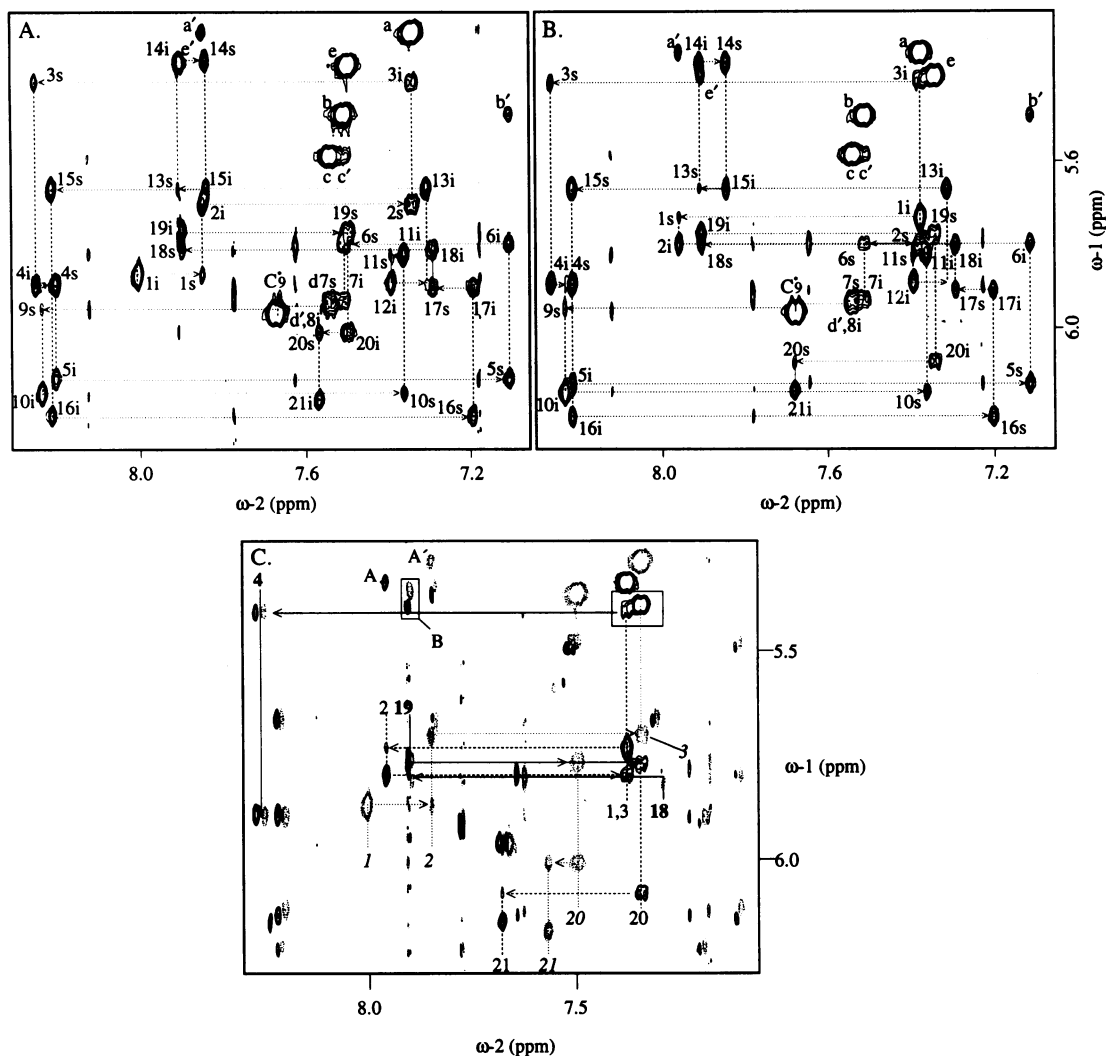
Figure 2. Expansions of NOESY spectra (τ_m = 200 ms) acquired in D_2O. This region contains the H6/8-H1' cross-peaks and are labeled as either intranuclear (i) or sequential (s) NOEs of the H1' protons (e.g. 15s indicates the sequential NOE between the H1' proton of residue G_{15} and the aromatic proton of A_{16}). Additional peaks that are not due to H6/8-H1' NOEs are labeled as follows: a, b, c, d and e indicate the intranucleotide H5–H6 NOEs for C_3, C_7, C_8, C_9 and C_{20} respectively; a', b', c', d' and e' indicate the G_2:H8–C_3:H5, T_6:H6–C_7:H5, C_7:H6–C_8:H5, C_8:H6–C_9:H5 and G_{19}:H8–C_{20}:H5 cross-peaks respectively. The peak labelled C_9^* contains the following cross-peaks overlapped: C_9:H5–C_9:H6, C_9:H1'–C_9:H6 and C_8:H1'–C_9:H6. The H2 protons of adenine give rise to several weak peaks with narrow ω-2 resonances that are not labeled. (A) Hairpin 1. (B) Hairpin 2. (C) A difference spectrum obtained by subtracting the spectral regions of parts (A) and (B). The NOESY experiments were reprocessed with extensive zero-filling in order to construct the difference spectrum, so that the expansion nearly fills a 2k × 2k matrix. The negative peaks are from 1 and the positive peaks are from 2. Due to small chemical shift changes some peaks that do not cancel completely remain as weak positive and negative lobes of equal intensity. The spectra are labelled according to the residue number of the aromatic proton (H6/H8). The NOE connectivity network of 1 is traced with dotted lines and the network of 2 is traced with dashed lines. Where the connectivity network for each hairpin overlaps, a solid line is used. Only the aromatic peaks for residues within three basepairs of the cross-link are labelled for clarity. The intranucleotide cross-peaks between G2:H8 and C3:H5 for 1 and 2 are labelled A' and A, respectively. The boxed region labelled B contains the residual peak volumes from the cross-peaks between the G19:H8 and C20:H5 protons of both hairpins. The unlabelled box contains too many overlapping signals to be interpreted.

proportional to the cross relaxation rate, σ, after correction for the short relaxation delay. The distance constraints then were calculated as follows (49):

$$r_{ij} = (A_{0ref} C_{ref} / A_{0ij} C_{ij})^{1/6} *r_{ref} \qquad (2)$$

where C is the correction factor for the short recycle delay. The cytosine H5–H6 interproton distance (2.48 Å) (50) was taken as the reference distance. The upper and lower distance bounds were calculated by carrying out the above calculations using twice the

standard deviation of the curve fits and an estimated error for the correction factor. For all proton pairs which involved a methyl proton another 1 Å was added to the upper bound.

RESULTS AND DISCUSSION

^{1}H resonance assignments

The non-labile proton resonances were assigned from DQF-COSY, TOCSY and long mixing time NOESY spectra measured in D_2O

Table 1. (A) Proton and phosphorus chemical shifts (10 °C, pH 7)

Base	H1'	H2'	H2"	H3'	H4'	H5'/5"	H5/5M/2	H6/8	31P	imino	amino
A1	5.94	2.48	2.62	4.82	4.19	3.67	7.92	8.01			
G2	5.77	2.25	2.25	4.96	4.36	4.16/4.09		7.85	-4.18	12.88	
C3	5.47	1.97	2.34	4.82	4.16		5.36	7.35	-4.22		6.36/8.30
A4	5.97	2.79	2.94	5.07	4.42	4.14/4.03	7.19	8.26	-4.01		
A5	6.19	2.59	2.93	5.00	4.49		7.63	8.21	-4.23		
T6	5.86	2.04	2.50	4.84	4.21		1.32	7.11	-4.41	13.64	
C7	6.00	2.09	2.49	4.83	4.15		5.55	7.51	-4.22		6.83/8.31
C8	6.00	2.20	2.45	4.76	4.15		5.66	7.55	-4.22		7.11/8.61
C9	6.04	2.06	2.44	4.74	4.26	3.94/3.80	6.04	7.68	-3.68		
A10	6.23	2.67	2.67	4.79	4.32	3.94/3.96	8.13	8.24	-4.14		
T11	5.89	1.99	2.24	4.67	4.07	4.01	1.43	7.37	-4.41		
T12	5.97	2.14	2.33	4.69	4.05	3.89/3.85	1.63	7.40	-4.39		
T13	5.73	1.85	2.16	4.66	4.12	3.95/3.91	1.74	7.32	-4.29		
G14	5.42	2.72	2.72	4.93	4.30	4.02/3.95		7.91	-4.20	13.15	
G15	5.74	2.69	2.81	5.03	4.42	4.25		7.85	-3.85	12.73	
A16	6.28	2.68	2.97	5.04	4.50		7.78	8.22	-4.31		
T17	5.98	2.02	2.56	4.85	4.21	4.32	1.28	7.20	-4.44	13.78	
T18	5.89	2.10	2.47	4.90	4.16	4.19/4.09	1.58	7.30	-4.45	13.82	
G19	5.83	2.70	2.70	4.99	4.40	4.12		7.90	-4.23	12.64	
C20	6.07	2.22	2.47	4.74	4.23	4.16	5.43	7.50	-3.85		6.72/8.31
T21	6.25	2.28	2.28	4.55	4.05	4.17/4.14	1.71	7.56			

Table 1. (B)

Base	H1'	H2'	H2"	H3'	H4'	H5'/5"	H5/5M/2	H6/8	31P	imino	amino
T_1	5.80	1.78	2.27	4.66	4.07	3.67	1.74	7.38			
G_2	5.87	2.65	2.72	4.94	4.33	3.98,4.07		7.96	-4.26	13.03	
C_3	5.48	1.99	2.34	4.82	4.16	4.17/4.07	5.41	7.38	-4.38		6.48/8.45
A_4	5.96	2.81	2.94	5.07	4.43	4.13,4.04	7.23	8.27	-3.98		
A_5	6.20	2.59	2.94	5.01	4.49		7.64	8.22	-4.22		
T_6	5.86	2.05	2.49	4.84	4.19		1.33	7.11	-4.43	13.64	
C_7	6.00	2.08	2.47	4.83	4.15		5.56	7.51	-4.22		6.83/8.33
C_8	6.01	2.19	2.45	4.77	4.15		5.65	7.54	-4.22		7.11/8.61
C_9	6.03	2.05	2.43	4.75	4.26	3.81,3.94	6.03	7.68	-3.69		
A_10	6.22	2.66	2.66	4.79	4.32		8.13	8.24	-4.14		
T_11	5.89	1.99	2.23	4.66	4.06		1.43	7.36	-4.42		
T_12	5.96	2.14	2.32	4.69	4.04		1.63	7.39	-4.40		
T_13	5.74	1.84	2.16	4.66	4.11	4.12	1.74	7.31	-4.30		
G_14	5.43	2.72	2.72	4.94	4.30	4.02,3.96		7.91	-4.21	13.15	
G_15	5.73	2.68	2.81	5.03	4.42	4.14		7.84	-3.86	12.73	
A_16	6.28	2.68	2.97	5.04	4.50	4.32	7.78	8.22	-4.34		
T_17	5.98	2.01	2.56	4.85	4.21		1.29	7.20	-4.45	13.78	
T_18	5.87	2.07	2.45	4.89	4.14		1.60	7.29	-4.45	13.88	
G_19	5.84	2.65	2.65	4.99	4.37	4.12		7.91	-4.20	12.76	
C_20	6.15	1.91	2.18	4.81	4.18		5.46	7.34	-3.91		6.80/8.31
T_21	6.22	2.26	2.30	4.51	4.04		1.87	7.68	-3.76		

The proton chemical shifts are referenced to H_2O at 4.95 p.p.m. and the ^{31}P data are relative to an external standard of TMS. (A) Hairpin 1. (B) Hairpin 2.

using the procedures reviewed by Wüthrich (Table 1A; 51). The NOESY cross-peak pattern of **1** is typical of B-DNA throughout the stem duplex with some variation observed in the loop (Figs 2 and 3). All of the glycosidic torsion angles are *anti* as indicated by the lack of strong intranucleotide aromatic to H1' NOESY cross-peaks. The H2' and H2" protons were stereospecifically assigned based on the relative intensity of the H1' to H2' and the H1' to H2" cross-peaks in a short mixing time NOESY experiment. The five adenine H2 protons were readily assigned on the basis of their long longitudinal relaxation times (~4 s versus an average of 1.8 s for this molecule) and from the imino proton data (*vide infra*). The H2 proton of A10 was assigned based on NOESY cross-peaks with the methyl protons of T11, T12 and T13.

To assign the labile protons of **1**, the cytosine amino protons were first identified from NOESY cross-peaks using the previously assigned cytosine H5 protons. The guanine imino

resonances were then identified by cross-peaks with the amino protons of base-paired cytosines. The thymidine imino protons were then assigned via sequential NOEs with the guanine imino protons. Watson–Crick hydrogen bonding extends from the penultimate residues (the terminal base-pair is frayed) through residues 8 and 14 which are immediately adjacent to the loop (Fig. 1). Hydrogen bonding of any sort was not observed in the loop, even when the spectra were measured at 1°C. The H2 protons of A4, A5 and A16 were assigned on the basis of their NOEs with the imino protons on the base-paired adenine and with both adjacent imino protons. The H2 proton resonance of A1 then was assigned since it was the only H2 proton resonance which could not be assigned to another proton.

The presence of the cross-link in **2** did not complicate the assignment of any of the labile or non-labile proton resonances and the procedure described above was not altered (Table 1B).
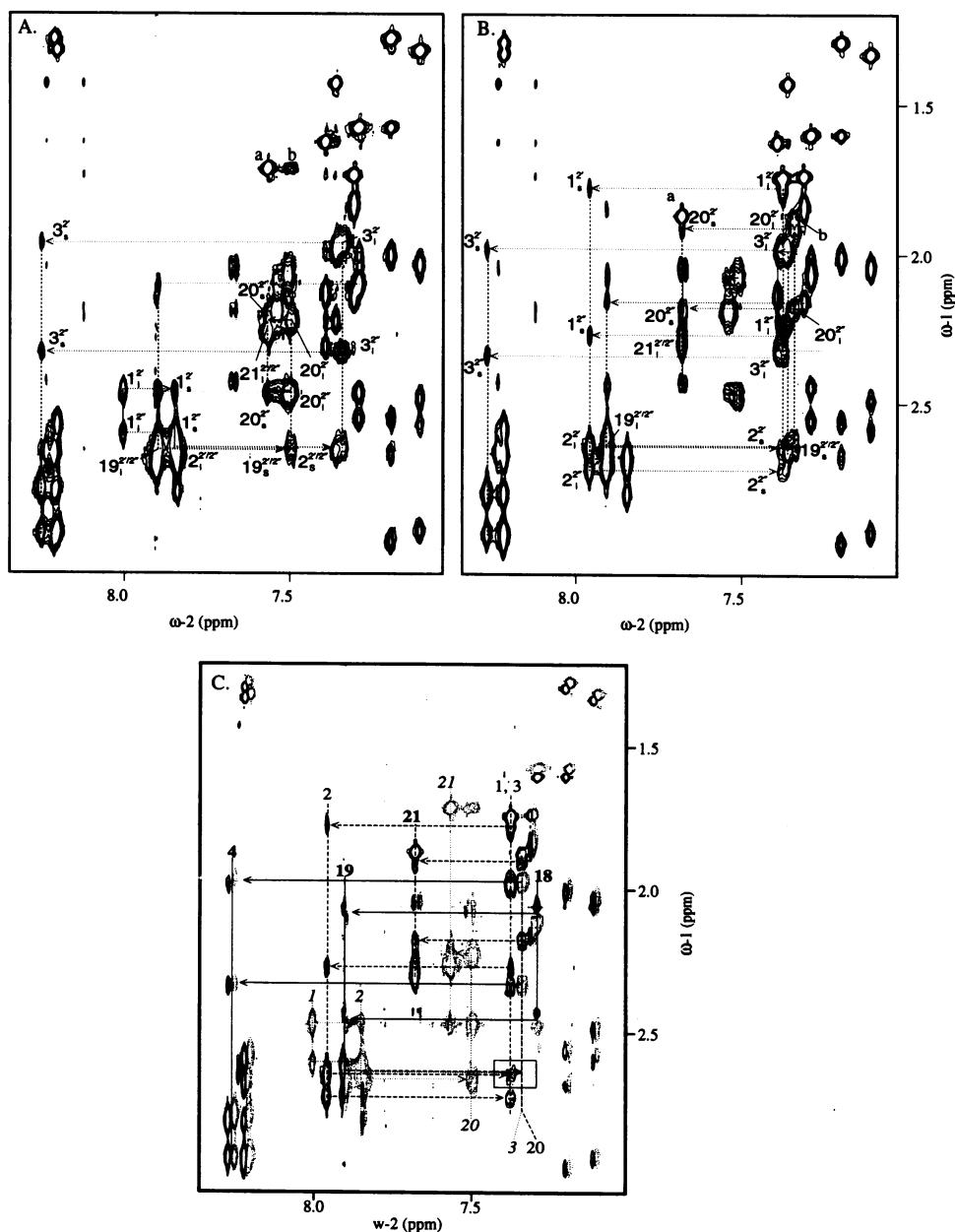
Figure 3. Expansions of NOESY spectra (τ_m = 200 ms) acquired in D_2O. This region contains the H6/8-H2′ and H6/8-H2″ cross-peaks. Peak labels for (A) and (B) are of the form X^y_x, where X is the residue number of the ω-1 resonance, y is the ω-1 proton type (i.e., 2′, 2″ or methyl), and z indicates whether the NOE is intranucleotide (i), sequential (s). (A) Hairpin 1. (B) Hairpin 2. (C) A difference spectrum obtained by subtracting the spectral regions of parts A and B, in the same manner used to make Figure 2C. The box contains a region where the intranucleotide peaks of C20:H6 of 1 and C3:H6 of 2 cancel nearly completely.

The protons of the cross link itself do not generate NOEs with any protons outside the cross-link and therefore cannot be assigned.

Spectral comparisons for 1 and 2

Overall, the non-labile proton spectra of 1 and 2 are quite similar. A ^1H chemical shift comparison of 1 and 2 is presented in Figure 4. When corresponding cross-peak volumes are compared (after a single scaling factor is applied to the volumes from one spectrum) none of the integratable peaks arising from within the set of protons in residues 3 through 19 differ in volume by more than experimental error. Subtraction of identically acquired NOESY

spectra allows comparison of the spectra without integration and in the presence of overlap within each spectrum (Figs 2C and 3C). Nearly complete self-cancellation is observed for cross-peaks involving the aromatic protons of the residues furthest from the cross-link, C8 through G14. Residues C3 through C8 and G15 through T18, which are located in the stem distal from the cross-link, afford residual peaks with lobes of equal positive and negative intensity, indicating that although chemical shifts of the protons differ, the NOE intensities do not. The C3:H6 cross-peaks of the two molecules are well separated in chemical shift but are of the same intensity. The cross-peaks arising from the H6/H8
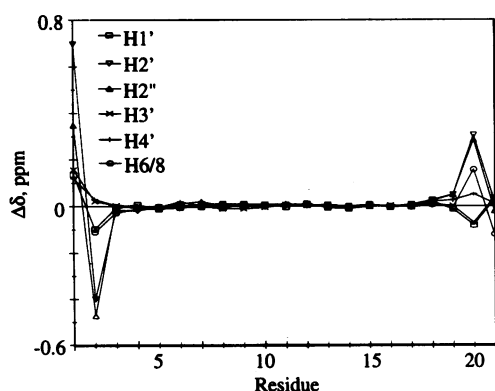
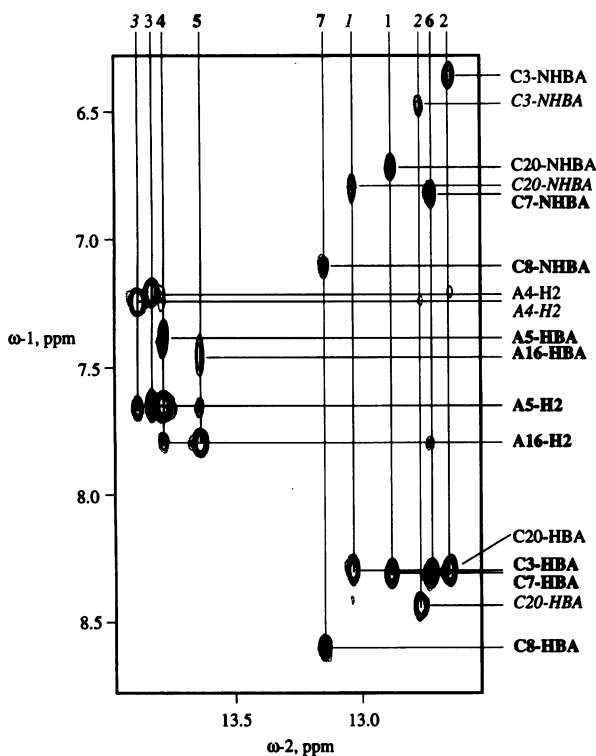**Figure 4.** Proton chemical shift comparison for 1 and 2.

Figure 5. Overlay of NOESY spectral expansions (τ_m = 200 ms) acquired in H$_2$O. The spectrum of **1** is rendered in black and the spectrum of **2** is grey. Assignments shown in bold apply to both molecules, assignments in plain text refer to **1**, and assignments in italics are unique to **2**. The imino protons are shown on the top axis and are labeled according to the number of base-pairs away from the cross-link (e.g. 1 refers to G2 of the penultimate base-pair). NHBA refers to non-hydrogen bonded amino protons, HBA refers to hydrogen bonded amino protons, and H2 refers to the adenine H2 protons.

resonances of the terminal two base pairs differ slightly in intensity suggesting that the terminal two base pairs of **1** and **2** may differ subtly, either structurally or with respect to local dynamics.

Overlays of NOESY spectra of **1** and **2** measured in 90% H$_2$O/10% D$_2$O are shown in Figure 5. The chemical shift values of the imino protons in both hairpins are remarkably similar, even for the protons that are proximal to the cross-link. In each case where differences are observed, the imino protons in **2** resonate
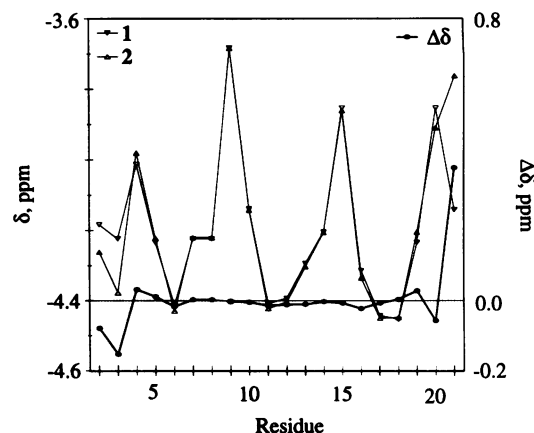

Figure 6. ^{31}P chemical shift comparison for 1 and 2. The chemical shift values are plotted relative to the left axis. The chemical shift differences, $\Delta\delta$, are plotted relative to the right axis. The approximate error is ± 0.01 p.p.m. for each measurement. It is improbable that any phosphates in either molecule adopt the B$_{II}$ conformation since such a conformation would be expected yield a chemical shift ~ 1.6 p.p.m. downfield of those observed for the typical B$_I$ conformation.

downfield of the corresponding protons in **1**. These data indicate that the disulfide cross-link does not disrupt canonical Watson–Crick base-pairing in the stem duplex. In fact, the finding that the hydrogen bonded imino protons near the terminus of **2** resonate downfield relative to the corresponding signals in **1** suggests that the cross-link may actually enforce base-pairing in the stem, perhaps by preventing end fraying.

Sugar pucker analysis

Due to self-cancellation of the COSY antiphase multiplets caused by wide line width, only the $^3J_{H1'-H2'}$, $^3J_{H1'-H2''}$ and $^3J_{H3'-H4'}$ multiplets are of sufficient intensity for coupling constant analysis. E-COSY spectra were used to extract $^3J_{H1'-H2'}$ and $^3J_{H1'-H2''}$, while the $^3J_{H3'-H4'}$ values were obtained by mixing vectors from COSY and NOESY spectra as described in the Materials and Methods section. The $^3J_{1H-1H}$ coupling constants indicate that the ribose rings of each residue in both hairpins, except for C20, exist predominatly in the C2' *endo* (South) conformation. The C20 puckering modes of both hairpins appear to be identical based on the unusual coupling data found for each molecule: $^3J_{H1'-H2'}$ = $^3J_{H1'-H2''}$ = 6.5. However, there are insufficient *J*-coupling data to conduct a detailed analysis of the North–South equilibrium.

Backbone analysis

The ^{31}P resonances of **1** and **2** were assigned based on internucleotide $^3J^{31}$P-H3' and intranucleotide $^4J^{31}$P-H4' cross-peaks in heteronuclear correlation experiments with previously assigned H3' and H4' protons. In B-DNA ^{31}P chemical shift values are very sensitive to backbone geometry and relatively insensitive to ring current effects, making them useful in the examination of backbone conformation (52). The difference in ^{31}P chemical shift between corresponding phosphates of **1** and **2** is small, relative to the chemical shift variation due to backbone heterogeneity within each molecule (Fig. 6). This finding indicates that our disulfide cross-link does not alter the backbone structure of duplex DNA and
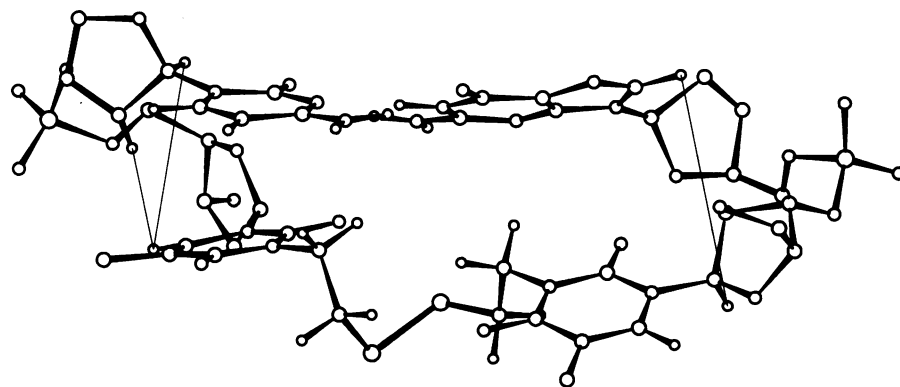
Figure 7. Ball and stick representation of the terminus of **2**. The narrow lines indicate corresponding inter-residue proton–proton distances that differ with respect to NOE-derived distances. Both the Intra-sugar proton–proton distances of residues 1 and 2 along with the G19:H1'–C20:H6 distance may vary slightly as shown by NOE build-up analysis. To derive this structure of **2**, restrained conjugate gradient energy minimization using the distance and torsion angle constraints were performed on the entire molecule. These calculations employed the AMBER (55,56) force field with reduced phosphate charges and reduced van der Waal radii. The minimization was conducted until the first derivative RMS was <0.1 kcal/Å^2. In this structure none of the distance constraints were violated by >0.1 Å. Similar results are obtained for **1** (data not shown).

is consistent with the results obtained from the proton spectra discussed above.

Loop structure

Several conclusions can be derived from the NMR data regarding the pentanucleotide loops in **1** and **2**. Between residues C9 and G14, only the A10 to T11 step yields the (strong) sequential NOEs expected for stacked B-DNA. The cross-peaks between the methyl groups of T11, T12 and T13 and the aromatic protons of A10, T11 and T12, respectively, are much weaker than expected for stacked B-DNA. The protons from all the sugars and bases in the loop afford the expected strong intraresidue NOEs. Only three NOESY cross peaks between protons on non-adjacent residues are observed, which are all caused by spin diffusion based on analysis of NOE build-up curves. Loops that fold into stable structures are often stabilized by unusual base pairs and exhibit direct NOEs between non-adjacent residues (53). Such NOEs are not observed for either **1** or **2**. In addition, NOEs that previously have been noted in hairpin loops which are stabilized by interaction with the minor groove are also not seen (53). Taken together, these data suggest that the loops in **1** and **2** do not adopt unique structures and are probably highly flexible.

Structure calculations and molecular modeling

Analysis of the NOE build up rates yielded 165 quantitative distance constraints for **1** and 185 for **2**. The contraints were flat well harmonic potentials with the range of the flat well determined by the error associated with the build-up rate analysis. This is a relatively small number of restraints per residue due to the problem of spectral overlap in these large oligomers. Thus, for the purposes of the structure calculations the base pairs were restrained to maintain the canonical hydrogen bond distance ±0.1 Å. Any peak caused by spin diffusion as judged by build-up curve analysis was constrained to be greater than the lowest bond length consistent with the build-up curve. In an attempt to constrain the loop protons to the maximum extent possible, a systematic search was made to identify each proton pair from the set of protons made up of the aromatic, H1', H2' and H2" protons

of residues 8 through 14 that did not give rise to an NOE. These proton pairs were assigned distance constraints >4.0 Å. In all cases we demonstrated that both of the protons gave rise to strong NOEs elsewhere in the spectrum, showing that the lack of NOE was not due to simple dynamic effects. A similar search for lack of NOEs was performed for the set protons contained in residues 1, 2, 20 and 21 for both molecules. Structures of **1** and **2** were derived using protocols involving distance geometry and simulated annealing, however due to insufficient restraints no method yielded a sufficiently tight family of conformers to make a high resolution structural comparison of **1** and **2**. Therefore, for purposes of visualization, Figure 7 presents a typical structure in which the corresponding inter-residue proton–proton distances that differ between **1** and **2** are indicated.

CONCLUSIONS

The experimental NOESY, ^{31}P and ^{1}H coupling constant and chemical shift data suggest that cross-link in **2** does not alter the structure of this hairpin relative to **1** such that **1** and **2** are isomorphous. That the cross-link in **2** does not disrupt native B-DNA geometry agrees with the results from an NMR study of another disulfide cross-linked DNA oligomer (22,54). In that work, however, the DNA sequence was a non-ground-state conformation whose unmodified counterpart could not be examined for comparison with the cross-linked analog. Thus, it is was not possible to unambiguously demonstrate that the cross-link is not structurally non-disruptive. Taken together, however, it appears that stabilizing oligodeoxyribonucleotides by incorporating our disulfide modification does not lead to major structural perturbations in native DNA geometry. Disulfide cross-linked oligomers such as these should therefore prove generally useful in studies of nucleic acid folding, structure and function.

ACKNOWLEDGEMENTS

REFERENCES

1 Cohen,L.F., Ewig,R.A.G., Kohn,K.W. and Glaubiger,D. (1980) *Biochim. Biophys. Acta*, **610**, 56–63.
2 Webb,T.R. and Matteucci,M.D. (1986) *J. Am. Chem. Soc.*, **108**, 2764–2765.
3 Leonard,N.J. and Devadas,B. (1987) *J. Am. Chem. Soc.*, **109**, 623–625.
4 Pieles,U., Sproat,B.S., Neuner,P. and Cramer,F. (1989) *Nucleic Acids Res.*, **17**, 8967–8978.
5 Millard,J.T., Raucher,S. and Hopkins,P.B. (1990) *J. Am. Chem. Soc.*, **112**, 2459–2460.
6 Lemaire,M.-A., Schwartz,A., Rahmouni,A.R. and Leng,M. (1991) *Proc. Natl. Acad. Sci. USA*, **88**, 1982–1985.
7 Cowart,M. and Benkovic,S.J. (1991) *Biochemistry*, **30**, 788–796.
8 Millard,J.T., Weidner,M.F., Kirchner,J.J., Ribeiro,S. and Hopkins,P.B. (1991) *Nucleic Acids Res.*, **19**, 1885–1891.
9 Kirchner,J.J. and Hopkins,P.B. (1991) *J. Am. Chem. Soc.*, **113**, 4681–4682.
10 Huang,H., Solomon,M.S. and Hopkins,P.B. (1992) *J. Am. Chem. Soc.*, **114**, 9240–9241.
11 Kirchner,J.J., Sigurdsson,S.T. and Hopkins,P.B (1992) *J. Am. Chem. Soc.*, **114**, 4021–4027.
12 Sigurdsson,S.T., Rink,S.M. and Hopkins,P.B. (1993) *J. Am. Chem. Soc.*, **115**, 12633–12634.
13 Boger,D.L. and Yun,W. (1993) *J. Am. Chem. Soc.*, **115**, 9872–9873.
14 Millard,J.T. and White,M.M. (1993) *Biochemistry*, **115**, 2120–2124.
15 Shi,Y.-b., Gamper,H. and Hearst,J.E., (1988) *J. Biol. Chem.*, **263**, 527–534.
16 Pinto,A.L. and Lippard,S.J. (1985) *Biochim. Biophys. Acta*, **780**, 167–180.
17 Tomasz,M., Lipman,R., Chowdary,D., Pawlak,J., Verdine,G.L. and Nakanishi,K. (1987) *Science*, **235**, 1204–1208.
18 Teng,S.P., Woodson,S.A. and Crothers,D.M. (1989) *Biochemistry*, **28**, 3901–3907.
19 Borowy-Borowski,H., Lipman,R. and Tomasz,M. (1990) *Biochemistry*, **29**, 2999–3006.
20 Ferentz,A.E. and Verdine,G.L. (1991) *J. Am. Chem. Soc.*, **113**, 4000–4002.
21 Glick,G.D. (1991) *J. Org. Chem.*, **56**, 6746–6747.
22 Glick,G.D., Osborne,S.E., Knitt,D.S. and Marino,J.P. Jr (1992) *J. Am. Chem. Soc.*, **114**, 5447–5448.
23 Ferentz,A.E., Keating,T.A. and Verdine,G.L. (1993) *J. Am. Chem. Soc.*, **115**, 9006–9014 and references therein.
24 Erlanson,D.A., Chen,L. and Verdine,G.L. (1993) *J. Am. Chem. Soc.*, **115**, 12583–12584.
25 Milton,J., Connolly,B.A., Nikiforov,T.T. and Cosstick,R. (1993) *J. Chem. Soc., Chem. Commun.*, 779–780.
26 Goodwin,J.T. and Glick,G.D. (1994) *Tetrahedron Lett.*, **35**, 1647–1650.
27 Goodwin,J.T., Osborne,S.E., Swanson,P.C. and Glick,G.D., (1994) *Tetrahedron Lett.*, **35**, 4527–4531.
28 Blatt,N.B., Osborne,S.E., Cain,R.J. and Glick,G.D. (1993) *Biochimie*, **75**, 433–441.
29 Swanson,P.C and Glick,G.D., (1993) *BioMed. Chem. Lett.*, **3**, 2117–2118.
30 Swanson,P.C, Cooper,B.C. and Glick,G.D., (1994) *J. Immunol.*, **152**, 2601–2612.
31 Tomic,M.T., Wemmer,D.E. and Kim,S.-H. (1987) *Science*, **238**, 1722–1725.
32 Marion,D. and Wüthrich,K. (1983) *Biochem. Biophys. Res. Commun.*, **113**, 967–974.
33 States,D.J., Haberkorn,R.A. and Ruben,D.J. (1982) *J. Magn. Reson.*, **48**, 286–292.
34 Marion,D., Mitsuhiko,I. and Bax,A. (1989) *J. Magn. Reson.*, **84**, 425–430.
35 Ernst,R.R., Bodenhausen,G. and Wokaun,A. (1987) *Principles of Nuclear Magnetic Resonance in One and Two Dimensions.* Oxford University Press, NY.
36 Piantini,U., Sørensen,O.W. and Ernst,R.R.. (1982) *J. Am. Chem. Soc.*, **104**, 6800–6801
37 Braunschweiler,L. and Ernst,R.R. (1983) *J. Magn. Reson.*, **53**, 521–528.
38 Rance,M. (1987) *J. Magn. Reson.*, **74**, 557–564.
39 Levitt,M.H., Freeman,R. and Frenkiel,T. (1982) *J. Magn. Reson.*, **47**, 328–330.
40 Griesinger,C., Otting,G., Wüthrich,K. and Ernst,R.R. (1988) *J. Am. Chem. Soc.*, **110**, 7870–7872.
41 Sklenář,V., Miyashiro,H., Zon,G., Miles,H.T. and Bax,A. (1986) *FEBS Lett.*, **208**, 94–98.
42 Plateau,P. and Guéron,M.. (1982) *J. Am. Chem. Soc.*, **104**, 7310–7311.
43 Griesinger,C., Sørensen,O.W. and Ernst,R.R. (1985) *J. Am. Chem. Soc.*, **107**, 6394–6396.
44 Sklenář,V. and Bax,A. (1987) *J. Am. Chem. Soc.*, **109**, 7525–7526.
45 Geen,H. and Freeman,R. (1991) *J. Magn. Reson.*, **93**, 93–141.
46 Titman,J.J. and Keeler,J. (1990) *J. Magn. Reson.*, **89**, 640–646.
47 Holak,T.A., Scarsdale,J.N. and Prestegard,J.H. (1987) *J. Magn. Reson.*, **74**, 546–549.
48 Denk,W. Baumann,R. and Wagner,G. (1986) *J. Magn. Reson.*, **67**, 386–390.
49 Reid,B.R., Banks,K., Flynn,P. and Nerdal,W. (1989) *Biochemistry*, **28**, 10001–10007.
50 Saenger,W. (1984) *Principals of Nucleic Acid Structure.* Springer-Verlag, Berlin.
51 Wüthrich,K. (1986) *NMR of Proteins and Nucleic Acids.* John Wiley & Son, NY.
52 Gorenstein,D.G. (1994) *Chem. Rev.*, **94**, 1315–1338
53 Hilbers,C.W., Heus,H.A., van Dongen,M.J.P. and Wijmenga,S.S. (1994) In Eckstein,F and Lilley,D.M.J. (eds), *Nucleic Acids and Molecular Biology.* Springer-Verlag, Berlin. Vol. 8, pp. 56–104.
54 Wang,H., Zuiderweg,E.R.P. and Glick,G.D. (1995) *J. Am. Chem. Soc.*, in press.
55 Weiner,S.J., Kollman,P.A., Case,D.A., Singh,U.C., Ghio,C., Alagona,G., Profeta,S. Jr and Weiner,P. (1984) *J. Am. Chem. Soc.*, **106**, 765–784.
56 Weiner,S.J., Kollman,P.A., Nguyen,D.T. and Case,D.A. (1986) *J. Comp. Chem.*, **7**, 230–252.